Journal of Applied Polymer Science

Effect of convergent-divergent flow on thermal and crystallization properties of PP/MWCNTs nanocomposites

Xiaochun Yin,[1] Zhongwei Yu,[1] Guizhen Zhang,[1] Zhitao Yang,[1] Baiping Xu[2]
[1]Key Laboratory of Polymer Processing Engineering of Ministry of Education, South China University of Technology, Guangzhou, China, 510640
[2]Department of Light Industry and Chemical, Guangdong Industry Technology College, Guangzhou, China, 510300
Correspondence to: Guizhen Zhang (E-mail: guizhenzhang@scut.edu.cn)

ABSTRACT: A melt-mixing process based on convergent–divergent flow has been used to prepare PP/MWCNT composites with a self-built convergent–divergent die (C-D die) composed of different numbers of convergent plates. Dynamic extensional deformation was generated in the C-D die, which improved the mixing effect and mixing efficiency of the composites during extrusion. The C-D die acted as a mixer for composites when mounted onto a capillary rheometer. The residence time of PP/MWCNTs melt in the extensional flow field is adjusted by changing the numbers of convergent plates and the velocity of the ram. The intensity of extensional flow field is controlled by the structure of the convergent plate and the ram velocity. Influences of convergent–divergent flow on PP/MWCNTs composites were characterized in terms of transmission electron microscopy (TEM), differential scanning calorimetry (DSC), and thermogravimetric analysis (TGA). TEM results showed that MWCNTs disperse more homogeneously with the increase of convergent plates. DSC showed that the crystallinity of PP/MWCNTs composites increased and the crystallization temperature shifted to higher temperature with the increase of the numbers of the convergent plates. TGA showed that the thermal stability of composites improved remarkably. The decomposition temperature increases from 381 to 408.2°C when the numbers of convergent plates increased from 2 to 8. In addition, the increase of ram velocity also has the same influences on the dispersion of MWCNTs in the resin and the properties of PP/MWCNTs nanocomposites. © 2015 Wiley Periodicals, Inc. J. Appl. Polym. Sci. **2015**, *132*, 42330.

KEYWORDS: composites; crystallization; degradation; extrusion; morphology

Received 12 January 2015; accepted 7 April 2015
DOI: 10.1002/app.42330

INTRODUCTION

Polymeric nanocomposites can be prepared by different routes, including in situ polymerization, solution processing, and melt mixing.[1] The latter, melt mixing, is a common method to acquire materials with specific properties based on the components used. From an industrial point of view, it is also an economically viable way to obtain specific materials, rather than synthesizing them. Melt mixing may use different kinds of equipment. At industrial scale, twin screw extruders of the co-rotating type became popular.[2] Laboratory R&D is generally based on the use of internal batch mixers and micro-compounders,[3,4] but prototype equipment is also frequently used.[5–7]

Most mixers and plastic processing machines mainly operate in shear flow field. However, it had been theoretically shown that mixing process dominated by extensional flow has many advantages such as well dispersion, reduced mixing temperature, and wide adaptability.[8] Taylor[9] introduced the deformation/break-up/coalescence mechanisms of dispersed droplets during the polymer mixing. It has been extensively studied by many researchers. Grace[10] has shown that the critical capillary number (Ca_{crit}), which controls the drop break-up process strongly rely on the flow pattern (shear or extensional flow) involved during melt blending. The main conclusion obtained by him was that the extensional flow field has a higher efficiency for dispersive mixing than shear flow field. Utracki *et al.*[11] designed a mixer dominated by extensional flow field, which can be used in industrial mixing process when attached to an extruder. Qu[12] invented a new type of nonscrew plasticizing processing equipment based on extensional deformation known as vane extruder. This equipment consists of certain groups of vane plasticizing and conveying unites and which can generate dynamic extensional deformation. Jia *et al.*[13] has shown that better mechanical properties and finer dispersion particles have been achieved because of the extensional flow field of vane extruder compared with those of the traditional twin-screw extruder.

The objective of this article is to illustrate the influences of convergent–divergent flow on the dispersion and thermal properties

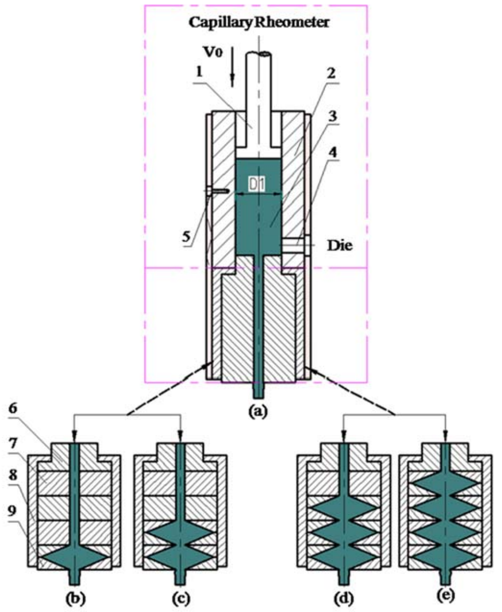

1-ram; 2-barrel, 3-materials, 4-pressure sensor, 5-thermocouple, 6-joint of die, 7-transition plate, 8-locating bush, 9-convergent plate
(a) 0 convergent plate, (b) 2 convergent plates, (c) 4 convergent plates, (d) 6 convergent plates, (e) 8 convergent plates

Figure 1. Melt mixers used in this work: a C-D die mounted on a capillary rheometer. [Color figure can be viewed in the online issue, which is available at wileyonlinelibrary.com.]

of PP/MWCNTs nanocomposites. A convergent–divergent geometry die has been built and tested to generate periodically changed extensional deformation. This die consisted of a series of convergent–divergent plates. It acted as a mixer when attached to a capillary rheometer. As the C-D die has mixing chamber of simple geometry, the cleaning is easy and the material lost is small. PP/MWCNTs nanocomposites were prepared in this equipment. And the influences of the numbers of convergent plates and extrusion velocity on morphology and thermal properties of composites were discussed.

EXPERIMENTAL

Materials

The based polymer for compound preparation was commercial PP from Maoming Petrochemical Co. with molecular weight of approximately 224 kg/mol and MFR of 10 g/min (200°C/2.16 kg). MWCNTs (purity:>96%), with a diameter between 10 to 15 nm and lengths ranging from 1 to 10 μm, was purchased from JCNANO Co., Nanjing, China. Although MWCNTs are difficult to disperse in polymer matrix because of the intrinsic strong inter-tubes Van der Waals interactions and the nature of hydrophobicity, the modification of MWCNTs are required. In this article, MWCNTs were incorporated under agitation into 68 wt % nitric acid for 3 h, then the modified MWCNTs suspension were filtered and dried at 90°C for 24 h in vacuum environment. The nitric acid–modified MWCNTs were obtained.[14]

Equipment

The mixing device used in this study is schematically represented in Figure 1. The mixing device is composed of a capillary rheometer and five types of die. The materials to be mixed were heated and melted in the barrel of the capillary rheometer. Materials were forced out from the die when the ram moves downward. As shown in Figure 1, four types of C-D dies were used in the experiments. The convergent and divergent flows dominated by extensional deformation in the C-D die are expected to contribute significantly to dispersive mixing.

Figure 2 shows the schematic diagram of material flow in transition plate and convergent plates of a C-D die. The gradient color in Figure 2(b) is to show the expansion and compression of the viscoelastic fluid. As shown in Figure 2(a), the flow type in a transition plate is steady laminar, materials

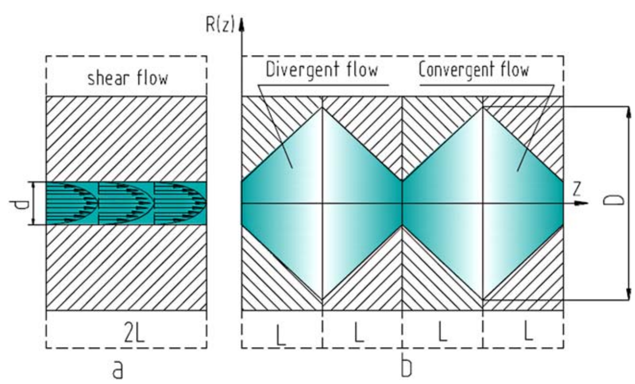

Figure 2. Flow field in convergent–divergent die. [Color figure can be viewed in the online issue, which is available at wileyonlinelibrary.com.]

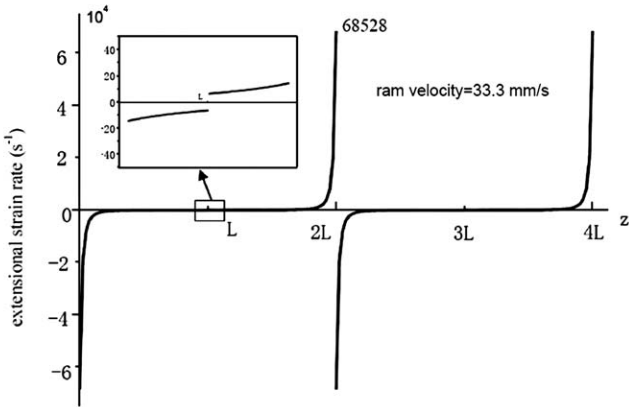

Figure 3. The extensional strain rate in the convergent–divergent die by numerical analysis.

suffers almost pure shear deformation. The wall shear rate can be estimated:[15]

$$\dot{\gamma}_w = \frac{8 \cdot D_1^2 \cdot V_0}{d^3}\frac{3n+1}{4n} \tag{1}$$

where D_1 is the diameter of the barrel, d is the diameter of small end of the convergent plate, V_0 is the velocity of the ram, and n is the flow rate index.

However, materials in the convergent region were accelerated because of the narrowing of the gap or slowed down in the diverging region because of the widening of the gap. This flow type creates strong extensional flow. The extensional deformation in the C-D die will change periodically when materials flow through the convergent plates. Jones and Binding[16] and Kim *et al.*[17] have used planar hyperbolic-shaped dies to analyze the extensional flow on the properties of polymer blends. As shown in Figure 2(b), the extensional strain rate $\dot{\varepsilon}$ can be estimated for an axi-symmetric geometry along the z-axis:

$$\dot{\varepsilon}(z) = \frac{d(v_z)}{dz} \tag{2}$$

where v_z is the average velocity at a given z. The expression of the volumetric flow rate Q is defined by:

$$Q = \pi \cdot R^2(z) \cdot v_z \tag{3}$$

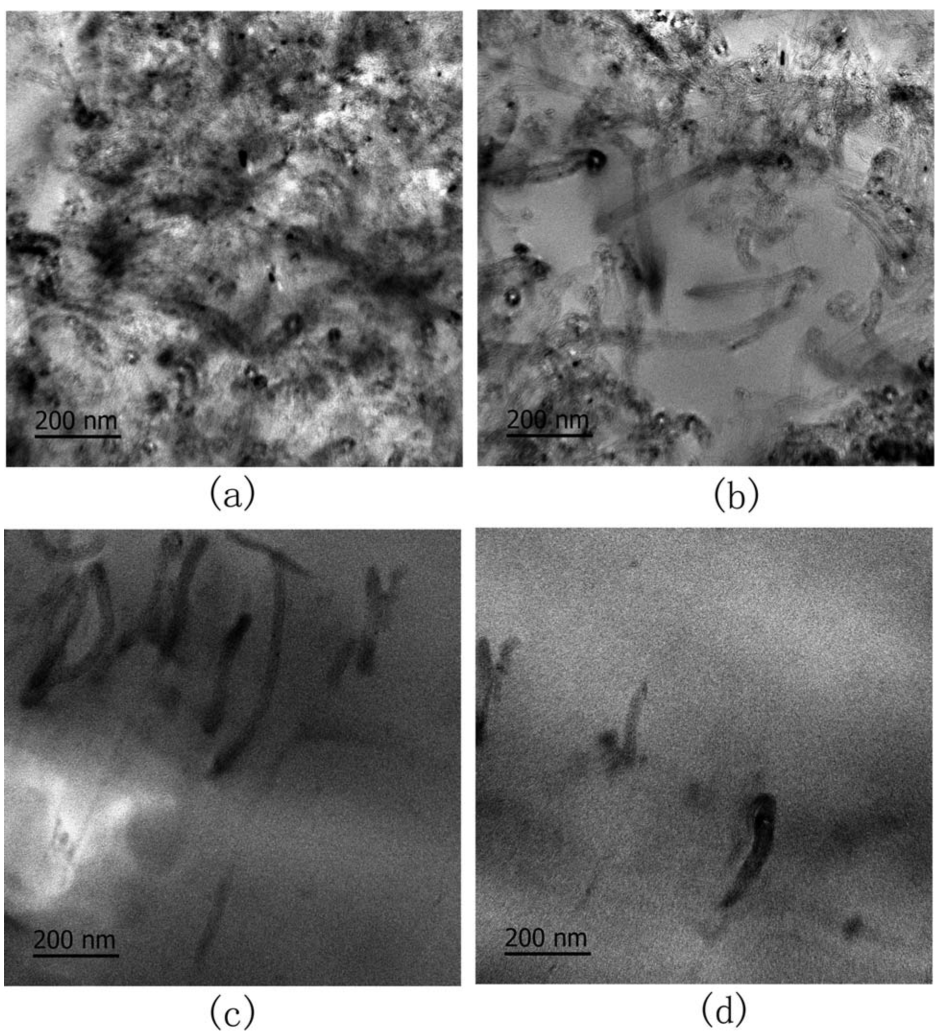

Figure 4. TEM images of PP/MWCNTs nanocomposites prepared with different dies; (a) 2 convergent plates, (b) 4 convergent plates, (c) 6 convergent plates, (d) 8 convergent plates.

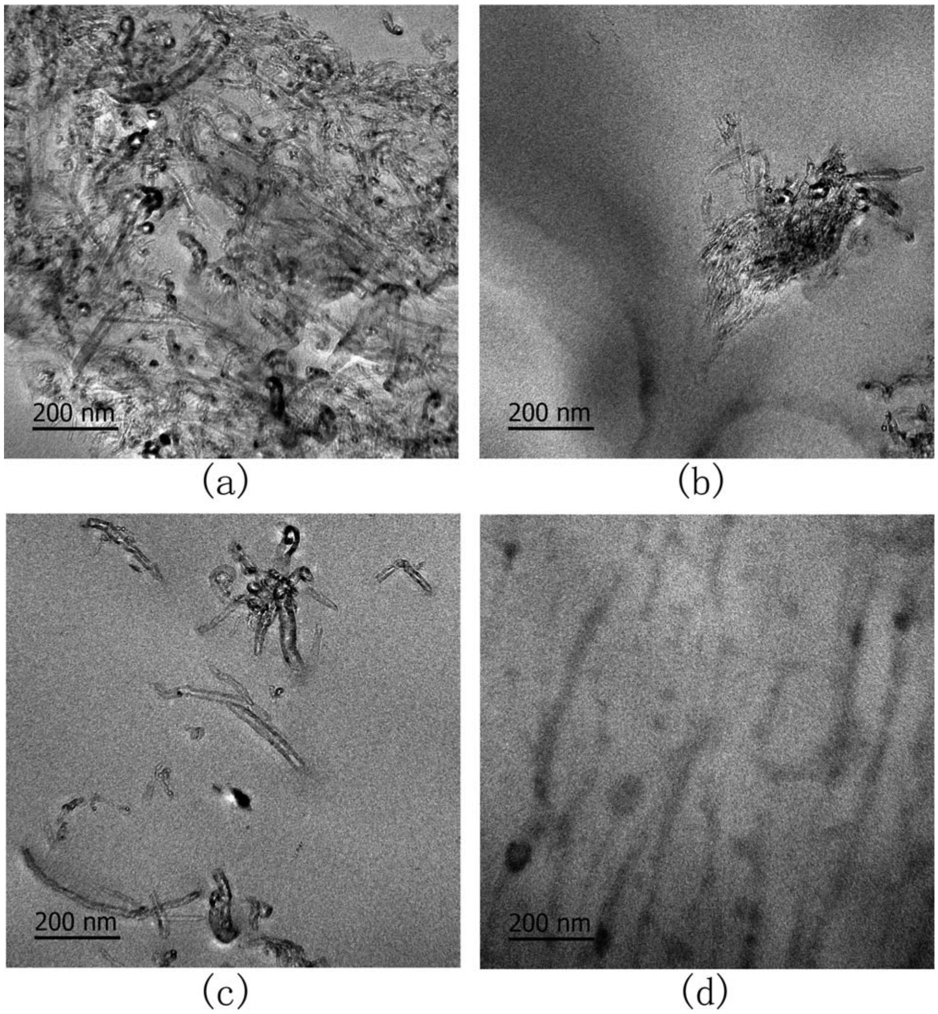

Figure 5. TEM images of PP/MWCNTs nanocomposites prepared at different ram velocity; (a) 27.8 mm/s, (b) 83.3 mm/s, (c) 166.7 mm/s, (d) 333.3 mm/s.

Also, the volumetric flow rate Q is determined by the ram velocity:

$$Q=\frac{\pi \cdot D_1^2 \cdot V_0}{4} \tag{4}$$

So, it can be deduced that:

$$\dot{\varepsilon}(z)=\frac{D_1^2 \cdot V_0}{4} \cdot \frac{d}{dz}\left(\frac{1}{R^2(z)}\right) \tag{5}$$

$R(z)$ can be calculated by:

$$R(z)=\begin{cases} \frac{D-d}{2l}z+\frac{d}{2}, & 0<z<l \\ \frac{d-D}{2l}(z-l)+\frac{D}{2}, & l<z<2l \end{cases} \tag{6}$$

For the self-built convergent–divergent die, the dimensions of the convergent plate and transition plate used in the experiments show as follows: The big-end diameter of the convergent flow channel D is 22 mm. The small-end diameter of the convergent flow channel d is 1 mm. The diameter of the barrel D_1 is 14 mm. The thickness of the convergent plate L is 4 mm.

According to eq. (6), we can calculate the extensional rate at given ram velocity. Figure 3 shows the change of extensional rate along direction when the ram velocity is 33.3 mm/s calculated by MATLAB. As shown in Figure 3, the extensional rate changes periodically along extrusion direction. Materials in the die suffers dynamic extensional deformation which can improve the fillers disperse more homogeneously in the matrix and enhance the orientation of the PP chains. As most of the polymeric materials are thermodynamically immiscible at a molecular scale, the extensional flow is beneficial to the shape of the phases and the nature of the interface between them.

Sample Preparation

Characterization

The PP/MWCTs nanocomposites with 1 wt % of MWCNTs were pre-mixed and then added into the barrel of capillary rheometer. The temperature of the barrel is set at 200°C. Five different dies (Figure 1) were used to process the materials. The ram velocity is 27.8mm/s, 83.3mm/s, 166.7mm/s, and 333.3 mm/s, respectively. The materials were preheated in the barrel for 2 min before extruded. The extrudate was collected

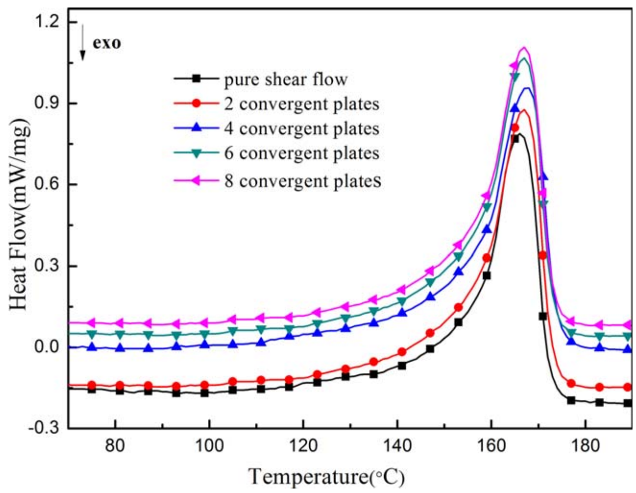

Figure 6. Melting curves of PP/MWCNTs prepared with different types of dies. [Color figure can be viewed in the online issue, which is available at wileyonlinelibrary.com.]

when the pressure of the inlet of the die is steady. The extrudate was fast cooled in liquid nitrogen.

The dispersion of MWCNTs in PP matrix was observed by transmission electron microscope (TEM, JEOL1011) at 200 kV accelerating voltage. Ultrathin slices are cryogenically cut using a Leica and a glass knife at −70°C. The specimens were collected on carbon-coated copper TEM grids.

Nonisothermal crystallization was performed by means of a differential scanning calorimeter (DSC) with DSC 204C instrument from NETZECH Co., German. The procedure performed in scans was the following: samples of about 3–6 mg were placed in an aluminium pan and were heated from 30 to 200°C at a scan rate of 10°C/min. Before cooling to room temperature samples were maintained for 3 min at 200°C to erase the thermal history. Then, samples were cooling down at the same scan rate from 200°C to room temperature under nitrogen gas to obtain the melting and crystallization temperature of the PP/MWCTs. The crystallinity X_c was calculated by the relative ratio of the enthalpy of crystallization per gram of samples to the heat of fusion of PP crystal.

TGA was performed to evaluate the thermal stability at high temperature with a NETZCH TG209 thermal analyzer. The samples about 3–5 mg were subjected were weighed and heated from room temperature (25°C) to 600°C at heating rate of 10°C/min under nitrogen atmosphere.

RESULTS AND DISCUSSION

Morphological Analysis

As we know, improvement on the property of PP/MWCNTs is attributed to MWNCTs dispersed homogeneously in PP matrix, which leads to fine interactions between PP chains and MWCNTs. Figure 4 shows the TEM microphotographs of PP/MWCNTs (1.0 wt %) nanocomposites prepared with different dies and this group of the experiment is performed under 83.8 mm/s ram velocity. It was shown in Figure 4 that the carbon nanotubes dispersed more homogeneously with the dies composed of more convergent plates at the same ram velocity.

As we know, the elongational flow is able to break-up, disperse, and orientate the particles of the dispersed system.[18] This does not occur in shear flow. The longer time the elongational flow imposed on the melt, the more apparent the effect is. In Figure 4, the whole residence time in flow field (shear flow and extensional flow) is unchanged at the same ram velocity. But the residence time in extensional flow field increased with the increase of convergent plates. The MWCNTs have enough time to move when the residence time is long which improved the dispersion properties of the MWCNTs in the matrix. As can been seen from Figure 4, when the C-D die composed of two convergent plates [Figure 1(b)] the residence time of the materials in extensional flow field is the shortest. Therefore, the MWCNTs do not have enough time to move and the MWCNTs are aggregating severely in PP matrix.

For intermediate convergent plate [Figure 4(b,c)], an improving dispersion and some individual MWCNTs can be found. In those two photographs, convergent plate has increased and the residence time of the material in extensional flow field was longer than in two convergent plate. At the same time, the probability of the presence of aggregates has reduced. As the number of the convergent plates increase to 8 [Figure 4(d)] individual MWCNTs dispersed homogeneously in the matrix can be observed. As implied previously, this state has a positive effect on whole properties. From these four microphotographs, it is optimistically demonstrated that the convergent plate have a significant influence on the dispersion of MWCNTs in PP matrix.

Figure 5 is the TEM images of PP/MWCNTs nanocomposites prepared at different ram velocity. Those four samples are extruded out under four convergent plates. As can be seen from Figure 5, the faster the ram velocity is, the more homogeneous the MWCNTs dispersed in PP matrix. As described in eq. (5), the extensional rate is related to the ram velocity and the intensity of the extensional rate increases with the increases of the

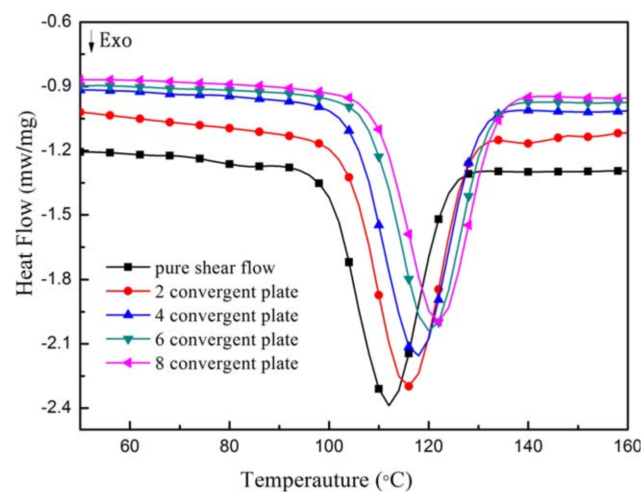

Figure 7. Nonisothermal crystallization exotherms of PP/MWCNTs prepared with different types of die. [Color figure can be viewed in the online issue, which is available at wileyonlinelibrary.com.]

Table I. Various Parameters of PP/MWCNTs Composites Determined from Nonisothermal Crystallization Exotherms Prepared with Different Types of Dies

Convergent plate	Crystallization peak T_c^P (°C)	Crystallization onset temperature T_{onset} (°C)	$T_{onset} - T_c^P$ (°C)	ΔH_m (J/g)	Melt peak T_m^P (°C)	Crystallinity X_c (%)
0	111.2	125.7	14.5	92.5	166.3	44.25
2	116.3	127.4	11.1	94.1	167.3	45.23
4	118.6	128.5	9.9	98.12	168.7	46.95
6	120.8	129.6	8.8	101.4	168.2	48.49
8	122.4	130.2	7.8	102.9	168.6	49.23

ram velocity. We know that extensional flow is beneficial to the dispersion efficiency of fillers. When a high intensity of extensional flow field imposed on the melt, the MWCNTs will suffer from a higher extensional force and the dispersed MWCNTs droplets will become smaller and dispersed homogeneously.

Crystallization Properties

Influence of the Numbers of the Convergent Plates on Crystallization Properties. Figures 6 and 7 show the melting curve and the crystallization curve of PP/MWCNTs composites with 1.0 wt % MWCNTs prepared with different dies, respectively. Those experiments are performed under 83.8 mm/s ram velocity. The melt peak temperature (T_m^P), the heat of fusion (ΔH), and crystallization onset temperature (T_{onset}) are summarized in Table I. The percentage of crystallinity (x_c) is calculated with equation:

$$x_c = \frac{\Delta H}{(1-\phi_p)\Delta H^0} \times 100\% \quad (7)$$

where ϕ_p is the weight fraction of filler in the composites, ΔH is the enthalpy measured of the analyzed sample (J/g), which is equal to the area below the melt peak of the melt curves, and ΔH^0 is a reference value that represents the heat of fusion for a 100% crystalline polymer. For PP, ΔH^0 is 209 J/g.[19]

It can be seen from Figure 6 that the melting peaks temperature of PP/MWCNTs nanocomposites prepared with C-D dies increased compared with that of prepared by pure shear flow. Also, we can see that the melting peaks of PP/MWCNTs nanocomposites prepared with C-D dies are wider than that of prepared by pure shear flow. This is because that some MWCNTs restricting molecular mobility of the polymer chains, so nanotube acts as obstacles to crystallization in some matrices.[20] As a result, the size of the crystals will differ from each other in the whole matrix, which makes the width of melting process wider.

It can be seen from Figure 7 that the crystallization onset temperature and the crystallization peak of PP/MWCNTs nanocomposites move to high temperature with the increase of the number of convergent plates. Table I confirms that the convergent–divergent flow in the C-D die leads to an increase in the crystallization temperature and crystallinity compares to pure shear flow. The relative shift of the T_c^P and the crystallinity are gradual increased with the increase of the convergent plates. On one hand, the residence time is longer when the number of the convergent plates increased, which will make MWCNTs dispersed more homogeneously in PP matrix; MWCNTs will act as nucleating agents for PP and enhance the crystallization rate and promotes the formation of inter-crystalline links[21]; on the other hand, the direction of the elongational stress and materials flow are almost same in the elongation flow, this will be helpful for the orientation of the polymer chain and increase the local order of matrix. As described by Green,[22] extensional

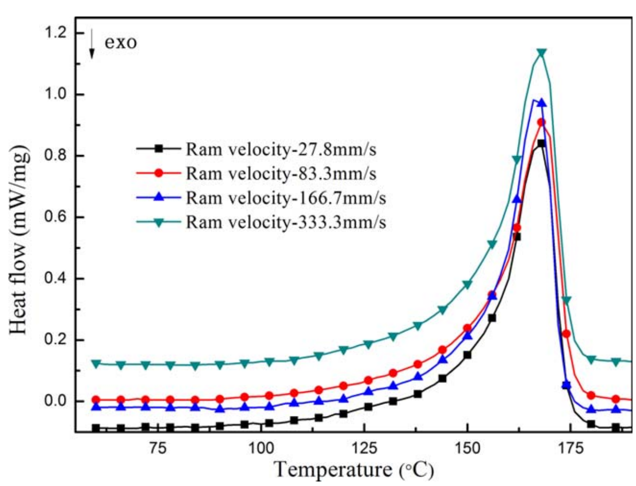

Figure 8. Melting curves of PP/MWCNTs prepared with different ram velocity. [Color figure can be viewed in the online issue, which is available at wileyonlinelibrary.com.]

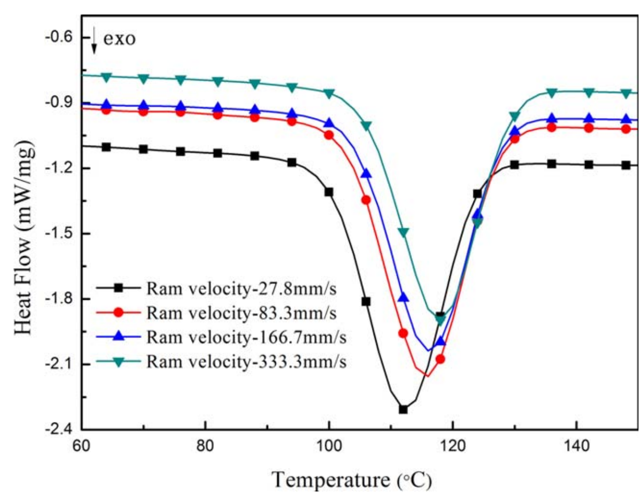

Figure 9. Nonisothermal crystallization exotherms of PP/MWCNTs prepared with different ram velocity. [Color figure can be viewed in the online issue, which is available at wileyonlinelibrary.com.]

Table II. Various Parameters of PP/MWCNTs Composites Determined from Nonisothermal Crystallization Exotherms Prepared with Different Ram Velocity

Ram velocity (mm/s)	Crystallization peak temperature T_c^p (°C)	Crystallization onset temperature T_{onset} (°C)	$T_{onset} - T_c^p$ (°C)	ΔH_m (J/g)	T_m^p (°C)	Crystallinity X_c (%)
27.8	112.4	126.9	14.5	97.42	167.5	46.61
83.3	114.2	127.5	13.3	98.21	168.5	46.99
166.7	115.3	128.2	12.9	101.2	167.6	48.42
333.3	117.9	128.7	10.8	103.9	168.9	49.71

deformation generated by the convergent–divergent flow in the C-D die is able to stretch the molecule increasing the local order and promoting the lamellae formation which causes a decrease of chain entropy, and, in turn, an increase of crystallization kinetics.

Influence of the Ram Velocity on Crystallization Properties. The extrusion velocity was directed influenced by the ram velocity. The shear/extensional rate in the die will increase with the increase of ram velocity when the structure of the die is constant. Figures 8 and 9 show the cooling and heating curves of PP/MWCNTs nanocomposites with 1.0 wt % MWCNTs prepared at different ram velocity respectively (convergent plate is 4). The corresponding thermal parameters are included in Table II.

As can be seen from Figures 8 and 9, the melting peak and crystallization peak shift to high temperature with the increase of the ram velocity. The width of the crystallization process is narrower which implying the growth of the crystals is accelerated, and thus, the overall crystallization rate rises. As seen from Table II, the crystallization peak changed from 112.4 to 117.9°C and the crystallinity increased from 46.61% to 49.71% when ram velocity increases from 27.8 to 333.3 mm/s. Equation (5) shows the extensional strain rate $\dot{\varepsilon}$ is positive to the ram velocity. That's to say, the extensional strain rate was determined by the ram velocity in the same die. The extensional rate increased with the increase of the ram velocity. The increase of extensional rate improved the dispersion of MWCNTs in PP matrix and the orientation of the PP chains which in turn improved the crystallization properties.

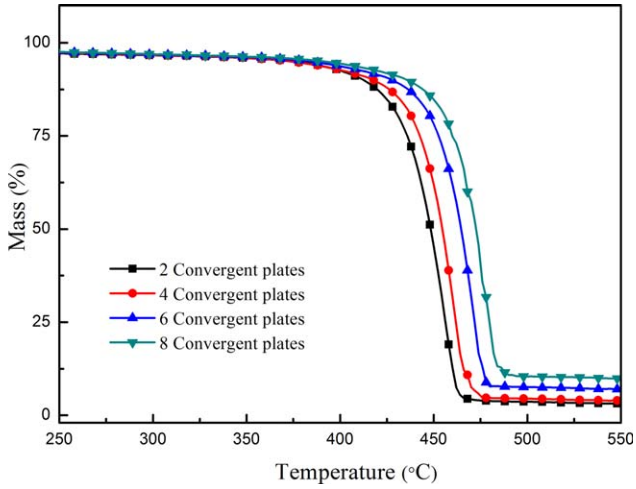

Figure 10. TGA thermograms curves of PP/MWCNTs prepared with different types of dies. [Color figure can be viewed in the online issue, which is available at wileyonlinelibrary.com.]

Thermal Stability

Influence of the Numbers of the Convergent Plates on Thermal Stability Properties. A comparative TGA of PP/MWCNTs prepared by different dies was shown in Figure 10 and the corresponding data was given in Table III. These samples are extruded out under 166.7 mm/s. As can be seen from Figure 10 and Table III, the introduction of convergent–divergent flow not only produced retardancy on oxidation temperatures but also on polymer decomposition at high temperatures. The onset degradation temperature increased from 381 to 408°C when the number of convergent plates increased from 2 to 8. Similar behavior can be noticed for final degradation temperature. Furthermore, as shown in Table III, the final residue remains increased from 3.11 to 9.89% when the numbers of the convergent plates increased from 2 to 8, which indicates that PP is carbonized by MWCNTs more severely.

The increase in the decomposition temperature of the PP/MWCNTs is due to the barrier effect of the carbon nanotubes, which form a barrier that obstructs the nitrogen diffusion, thus retarding the degradation of polypropylene as described by Gong *et al.*[23] The higher degradation temperature is related to the better dispersion of MWCNTs. The enhanced thermal stability can also be explained if we take into account the role of MWCNTs, they can establish some interaction with PP matrix and form a network's structure which is responsible for mobility restriction of PP chain.[24]The more homogeneous the MWCNTs dispersed in PP matrix, the denser the network is. When polymer chains are difficult to move, it indicates that the materials have higher thermal stability. As can been seen from Figure 4,

Table III. Degradation Temperatures of PP/MWCNTs Composites Prepared with Different Types of Dies

Convergent plate	T_{onset} (°C)	T_{final} (°C)	TGA final residue (%)
2	381.0	474.1	3.11
4	387.1	477.3	3.91
6	391.2	485.2	7.01
8	408.2	488.6	9.89

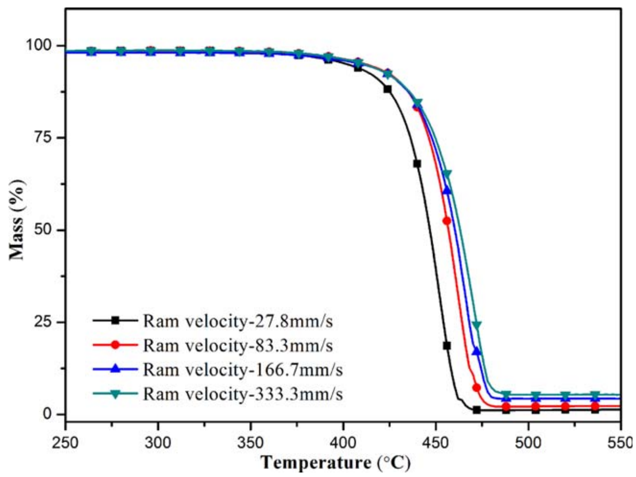

Figure 11. TGA thermograms curves of PP/MWCNTs prepared with different ram velocity. [Color figure can be viewed in the online issue, which is available at wileyonlinelibrary.com.]

the MWCNTs homogeneously disperse in PP matrix. Thus the thermal stability is improved.

Influence of the Ram Velocity on Thermal Stability Properties. Influence of the ram velocity on thermal behaviors of PP/MWCNTs composites were presented in Figure 11 (convergent plate is 6). As can be seen from Figure 11, the curves move to high temperature with the increase of ram velocity. The corresponding data were summarized in Table IV.

The onset degradation temperature is about 385.3°C when the ram velocity is 27.8 mm/s, but the value increased up to 395.6°C when the ram velocity increased to 333.3 mm/s. The final degradation temperature and TGA final residue are also increased with the increase of the ram velocity. As we described before, the extension strain rate has a close relation with the extrusion velocity. When the ram velocity increases, the extrusion velocity will increase which will increase the compression/extension stress imposed on the materials. The MWCNTs will disperse more homogeneously in PP matrix correspondingly. It is no doubt that the thermal stability of samples will be improved.

CONCLUSIONS

In this work, a new type of die based on convergent–divergent flow was designed and tested. Based on this custom-built C-D die, PP/MWCNTs were prepared by mounted the die onto a capillary rheometer. TEM microphotographs showed that the dispersion of MWCNTs is more homogeneously with the increase of the numbers of the convergent plates and the ram velocity. MWCNTs exhibited a good dispersion with more convergent plates or higher ram velocity. DSC results indicated the increase of the numbers of the convergent plates and ram velocity could improve the crystallization properties of PP/MWCNTs nanocomposites. For example, the crystallization temperature and crystallinity increased with the increase of convergent plate or extrusion velocity. TGA showed that convergent plate and extrusion velocity have an influence on thermal stability of PP/MWCNTs. The decomposition temperature moves to higher temperature, which implied the flame retardancy of PP/MWCNTs is better than before.

Table IV. Degradation Temperatures of PP/MWCNTs Composites Prepared with Different Ram Velocity

Ram velocity (mm/s)	T_{onset}(°C)	T_{final} (°C)	TGA final residue (%)
27.8	385.3	461.2	3.34
83.3	389.4	466.3	4.42
166.7	393.2	467.6	6.36
333.3	395.6	472.1	7.44

In this article, a mixer that based on extensional flow field has been design. This mixer has a small capacity, consuming small quantities of materials. Unlikely the traditional internal mixer or twin screw extruder, those device will consume large quantities of materials. The cost of the experiment in those device will be high. It will not suit to the nanocomposites because of the high price of the nanomaterials. In addition, the mixer that design in this experiment work on the principle of extensional flow field. We can have a deeply understanding of benefit of extensional flow from this technique. This technique not only provide us a method of self-reinforced materials, but also teach us mould design in industry area.

ACKNOWLEDGMENTS

The authors are thankful for the financial support received from Key Projects in the National Science & Technology Pillar Program during the Twelfth Five-year Plan Period (Project number 2011BAE15B01), Project on the Integration of Industry, Education and Research of Guangdong Province (2013B090600066), Project on the Integration of Industry, Education and Research of Dong Guan city, Guangdong Province (2014509105214), and the National Natural Science Funds (51403068).

REFERENCES

1. Breuer, O.; Sundararaj, U. *Polym. Compos.* **2004**, *25*, 630.
2. Eitzlmayr, A.; Koscher, G.; Reynolds, G.; Huang, Z. Y.; Booth, J.; Shering, P.; Khinast, J. *Int. J. Pharm.* **2014**, *474*, 157.
3. Sundararaj, U.; Macosko, C. W.; Nakayama, A.; Inoue, T. *Polym. Eng. Sci.* **1995**, *35*, 100.
4. Lin, B.; Sundararaj, U.; Potschke, P. *Macromol. Mater. Eng.* **2006**, *291*, 227.
5. Breuer, O.; Sundarafaj, U.; Toogood, R. W. *Polym. Eng. Sci.* **2004**, *44*, 868.
6. Maric, M.; Macosko, C. W. *Polym. Eng. Sci.* **2001**, *41*, 118.
7. Covas, J. A.; Costa, P. *Polym. Test.* **2004**, *23*, 763.
8. Osswald, T.; Gramann, P. New York: 57th SPEANTEC **1999**, 67.
9. Taylor, G. I. *Proc. R. Soc. London A* **1932**, *132*, 40.
10. Grace, H. P. *Chem. Eng. Commun.* **1982**, *14*, 225.

11. Utracki, L. A.; Luciani, A.; Bourry, D. J. J. W.O. Pat. 1999, 016,540 A2.
12. Qu, J. P. Eur. Pat. **2008**, 2,113,355 A1.
13. Jia, S. K.; Qu, J. P.; Liu, W. F.; Wu, C. R.; Chen, R. Y.; Zhai, S. F.; Huang, Z. *Polym. Eng. Sci.* **2014**, *54*, 716.
14. Peng, N. S.; Liu, W. J.; Liu, S. Y. *J. Ceramics* **2011**, *32*, 37 (in Chinese).
15. Xu, P. X. Polymer Rheology and its Application; Chemical Industry Press: Beijing, **2003**; pp 208.
16. Binding, D. M.; Jones, D. M. *Rheol. Acta* **1989**, *28*, 215.
17. Kim, H. C.; Pendse, A.; Collier, J. R. *J. Rheol.* **1994**, *38*, 831.
18. Utracki, L. A.; Sepehr, M.; Li, J. *Int. Polym. Process.* **2006**, *1*, 3.
19. Avalos, F.; Manchado, M.; Arroyo, M. *Polymer* **1996**, *37*, 5681.
20. Roumeli, E.; Markoulis, A.; Kryratsi, T.; Bikiaris, D.; Chrissafis, K. *Polym. Degrad. Stab.* **2014**, *100*, 42.
21. Martinez de Arenaza, I.; Sarasua, J. R.; Amestoy, H.; Lopez, R. N.; Zuza, E.; Meaurio, E.; Meyer, F.; Santos, J. I.; Raquez, J. M.; Dubois, P. *J. Appl. Polym. Sci.* **2013**, *130*, 4327.
22. Green, E. C.; Zhang, Y. Y.; Minus, M. L. *J. Appl. Polym. Sci.* **2014**, *131*, 40763.
23. Gong, J.; Tian, N. N.; Wen, X. *Polym. Degrad. Stab.* **2014**, *104*, 18.
24. Li, Y. A.; Yu, F. P.; He, W. J.; Yang, W. M. *J. Appl. Polym. Sci.* **2015**, *132*, 41234.